Algorithm and operational concept for resolving short-range conflicts

H Erzberger and K Heere

Proceedings of the Institution of Mechanical Engineers, Part G: Journal of Aerospace Engineering 2010 224: 225
DOI: 10.1243/09544100JAERO546

Algorithm and operational concept for resolving short-range conflicts†

H Erzberger[1]* and **K Heere**[2]
[1]Department of Electrical Engineering, University of California, Santa Cruz, California, USA
[2]University Affiliated Research Center, University of California, Santa Cruz, California, USA

The manuscript was received on 4 March 2009 and was accepted after revision for publication on 12 August 2009.

DOI: 10.1243/09544100JAERO546

Abstract: The article describes an algorithm for computing horizontal resolution trajectories with a limit on bank angle. If loss of separation can be avoided, the algorithm generates a set of manoeuvres that achieves or exceeds the specified minimum separation. The manoeuvres consist of turns to a specified heading followed by straight-line flight. Both single aircraft and cooperative manoeuvres are generated. In cooperative manoeuvres, both conflict aircraft simultaneously execute resolution manoeuvres, which expedite the resolution process compared to single aircraft manoeuvres. If loss of separation is unavoidable for a specified bank angle limit, the method chooses the manoeuvre that maximizes the minimum separation during the turns. The characteristics of the resolution trajectories have been analysed in a parameter space comprising initial positions, encounter angle, airspeed, predicted minimum separation, and bank angle. Analysis of resolutions for sets of initial conditions provided a road map for the design of an algorithm. The conceptual design of a system is described that resolves close-in conflicts automatically by uplinking resolution advisories to aircraft. Controllers have the option to assign detected conflicts to be resolved by the system. The system also has the authority to uplink resolution advisories to the aircraft without prior controller approval if time to loss of separation falls below a threshold value. The Mode S Specific Services data link is well suited for uplinking resolution advisories to the conflict aircraft. Deployment of the system could be an initial step in building the next-generation air traffic control system.

Keywords: air traffic management, automated conflict resolution, collision avoidance

1 INTRODUCTION

A fundamental design requirement for the next-generation air traffic control system is a highly reliable and safe method for automating separation assurance. Several independent and redundant systems for separation assurance are necessary to achieve that requirement. A candidate for the next-generation system, referred to as the automated airspace concept (AAC), incorporates two levels of protection against conflicts and one against collisions [**1**].

The first level, referred to as the autoresolver, is designed for resolving conflicts that are ∼2–30 min to first loss of separation. It provides the first line of defense against loss of separation and is intended to be the workhorse of the separation assurance system. In addition to resolving conflicts, the autoresolver also provides trajectory segments that return aircraft back to their original flight plans after the resolution segments of the trajectories have been completed. The design and performance of the autoresolver have been described in recent papers [**2**, **3**].

The second level of separation assurance handles conflicts that are not detected until loss of separation is <2 min away or, even if successfully detected, could not be resolved successfully by the first level. Conflicts detected close to loss of separation indicate a probable failure in the first level of conflict detection and resolution. Close-in conflicts can also arise when aircraft deviate unexpectedly from their

*Corresponding author: Department of Electrical Engineering, University of California, Santa Cruz, CA 95064, USA.
email: heinz.erzberger@nasa.gov

†*Major portions of this paper were presented at the 26th International Congress of the Aeronautical Sciences, Anchorage, Alaska, September 2008.*

planned trajectories. Although close-in conflicts are expected to occur infrequently, they pose a safety risk and therefore should be handled by an independent system specifically designed to resolve such conflicts. A system referred to as the tactical separation assured flight environment (TSAFE) is hypothesized in reference [**1**] for detecting and resolving these close-in conflicts. TSAFE would automatically take control of resolving close-in conflicts when the conflict detection element of TSAFE predicts that time to loss of separation has breached a critical time threshold. The design and performance of the detection element of TSAFE have been described in several papers [**4**, **5**].

In the AAC architecture, the third level of separation assurance is provided by the traffic advisory and collision avoidance system (TCAS). By Federal Aviation Administration (FAA) mandate, TCAS is required equipage in large passenger aircraft as well as in many other high-performance aircraft. It provides aural resolution advisories to pilots when a collision is predicted to occur within ∼20–35 s. In an operational implementation of AAC, TCAS alerts should become exceedingly rare, since they should occur only after both the autoresolver and TSAFE have failed to detect and resolve conflicts at earlier times.

This article focuses on the design of the resolution function of TSAFE, which is referred to as TSAFE Resolution. It first derives an analytical method for calculating the minimum separation of arbitrary resolution manoeuvres with limits on the turn rate. It then describes an algorithm designed specifically for resolving close-in conflicts in the horizontal plane.

The second part of the article describes an operational concept for shifting the responsibility for resolving close-range conflicts from controllers to TSAFE Resolution. This concept, which constitutes a paradigm shift in air traffic control, is proposed as a transitional step in building the next-generation system. Although TSAFE was originally designed to serve as a safety net for resolving conflicts at close range within the Advanced Airspace Concept, its potential as an independent system for resolving close-range conflicts with controllers remaining in the loop is investigated here. It is to be implemented in such a way that controllers retain their ability to manage traffic by conventional procedures. The concept has the potential to increase airspace capacity by allowing controllers to handle more traffic while committing fewer operational errors. TSAFE Resolution could be implemented in the National Airspace System (NAS) in the near term by using the Mode S Specific Services data link to uplink resolution advisories to the aircraft. Mode S is an operational technology that supports TCAS. Its use will reduce the cost of equipping aircraft to receive TSAFE Resolution advisories.

2 NEED FOR INCLUDING TURN RATE

A safe and effective method for resolving close-in conflicts in the horizontal plane must account for the finite turn rate of aircraft. The finite turn rate produces a horizontal-plane trajectory with a non-zero turn radius. When the turn radius becomes a significant fraction of the distance to the point of conflict, the method of computing the resolution trajectory must account explicitly for the achievable turn radius. Failure to do so could result in an unsafe manoeuvre that does not clear the conflict. This situation generally occurs when time to first loss is less than ∼2 min away. It is further exacerbated during encounters at high airspeeds. Since the turn radius increases with the square of the speed at a fixed bank angle, conflict encounters at high speed are especially susceptible to be affected by a bank angle limit.

Adaptation of the horizontal resolution algorithm built into the autoresolver was investigated for use in TSAFE. This algorithm first generates idealized resolution trajectories by a procedure that assumes that the conflict aircraft can change heading instantaneously [**2**]. An iterative procedure then corrects resolution failures resulting from this assumption. This is done by using a trajectory engine that includes turn dynamics to generate a flyable trajectory from specification of the idealized trajectory. If the flyable trajectory fails to resolve the conflict, the algorithm revises the idealized trajectory and repeats the process. For conflicts that are more than 2 min from loss of separation, the iteration procedure converges rapidly to a successful resolution trajectory that uses reasonable turn radii.

However, this method of compensating for instantaneous heading changes becomes inappropriate for close-range encounters when the time to turn with non-zero turn radius dominates the resolution manoeuvre. For such conditions the initial assumption of an idealized trajectory obscures and fails to reveal the complex behaviour of the separation characteristics during manoeuvres at close range. Thus, explicit modelling of the turn dynamics in the analysis of resolution trajectories is required in order to capture the full range of possible relationships between a conflict scenario and acceptable resolution manoeuvres. In previous work, Paielli [**6**] also developed an iterative procedure to compensate for turn dynamics. His procedure is more appropriate for resolving conflicts at longer range, namely those with more than 2 min to loss of separation. In reference [**7**], Mitchell *et al*. design a method for conflict resolution in which reachable sets are determined that represent all potential unsafe manoeuvres of the aircraft. Control laws, which include turn dynamics, are designed to ensure that the aircraft remain outside of these sets.

Another reason to include explicit modelling of turn dynamics is the need for TSAFE to be independent of any external and complex software functions such as a trajectory engine. The TSAFE resolution algorithm must be self-contained, simple in design, and targeted narrowly to resolve short-range conflicts. The algorithm presented in this article achieves these requirements by obviating the need for a separate trajectory engine and using computationally efficient procedures to generate resolution trajectories with bank angle constraints.

3 ANALYTICAL FORMULATION

The determination of resolution trajectories that meet specified separation criteria in the horizontal plane could be formulated as an optimum control problem, as was done in reference [**8**]. In such a formulation, the dynamical system would be given by a set of three differential equations

$$\frac{\mathrm{d}\psi}{\mathrm{d}t} = \frac{g\tan\phi}{V}, \quad \frac{\mathrm{d}x}{\mathrm{d}t} = V\sin\psi, \quad \frac{\mathrm{d}y}{\mathrm{d}t} = V\cos\psi \tag{1}$$

In these equations, ψ is the heading angle, g is the acceleration of gravity, V is the airspeed, and ϕ is the bank angle. The variables x and y are the position coordinates in a rectangular (stereographic pseudo-Cartesian) coordinate system. Since a separate set of these equations is required for each aircraft, the dynamical system for this control problem would thus be of sixth order. The bank angles for the two aircraft would be chosen as the control variables. If the speeds could also vary, then two differential equations with speeds as the state variables would have to be added to model the acceleration for each aircraft. In this article, it is assumed that the speeds are held fixed during the manoeuvre. This assumption is justified for short-range conflict resolution because aircraft typically respond too slowly to speed change inputs to make them effective for short-range resolutions.

Although it is possible to find a solution to the conflict resolution problem when formulated as an optimum control problem, the solution is difficult to implement in practice. Therefore, the approach taken in this article is to limit the resolution manoeuvres executed by each aircraft to control actions consisting of turns at a specified and fixed value of bank angle flown for a specified time interval, followed by straight-line flight (zero bank angle). Since each aircraft is also assumed to be holding its speed constant during these manoeuvres, the horizontal trajectories corresponding to this class of control actions consist entirely of circular arcs and straight-line segments. This assumption on the permitted control actions eliminates the need to solve differential equations altogether and simplifies the resolution trajectory calculations to a computationally more tractable algebraic problem. The resolution manoeuvres resulting from this formulation have the further advantage of being simple to specify to pilots and easy for them to fly.

The two aircraft involved in the conflict are referred to as A and B. Aircraft A is initially located at the origin of coordinates flying with speed V_A. The direction of the y-axis is chosen to be aligned with the initial heading of aircraft A. Thus, A has an initial heading of 0°. Aircraft B is initially located at coordinates $(x_{\mathrm{B}0}, y_{\mathrm{B}0})$ flying at speed V_B and heading $\psi_{\mathrm{B}0}$, which is measured clockwise with respect to the y-axis. The turn radii for each aircraft are determined by the following relations

$$R_\mathrm{A} = \frac{V_\mathrm{A}^2}{g\tan\phi}, \quad R_\mathrm{B} = \frac{V_\mathrm{B}^2}{g\tan\phi} \tag{2}$$

A resolution can be performed by manoeuvre of aircraft A by itself or B by itself or both A and B together. Manoeuvre of both aircraft to avoid a conflict is referred to as a cooperative resolution manoeuvre. A resolution manoeuvre is determined by specifying a turn direction, left or right, and a time interval for the aircraft to turn at the specified bank angle ϕ and then to resume straight-line flight. It is assumed that both aircraft will turn at the same bank angle for the same time interval if a cooperative resolution is chosen. Given a time to turn t, the resulting heading changes are determined as follows

$$\Delta\psi_\mathrm{A} = \frac{t\,g\tan\phi}{V_\mathrm{A}}, \quad \Delta\psi_\mathrm{B} = \frac{t\,g\tan\phi}{V_\mathrm{B}} \tag{3}$$

Note that if the two aircraft are flying at different speeds, their heading angles will change at different rates. For the analysis to follow, it is convenient to consider the absolute value of the heading-change angle of one of the two aircraft as the independent variable instead of time. Thus, if the absolute value of the heading change of aircraft A is chosen as the independent variable, then equations (3) above can be used to calculate the absolute value of heading change of aircraft B as follows

$$|\Delta\psi_\mathrm{B}| = \frac{V_\mathrm{A}}{V_\mathrm{B}}|\Delta\psi_\mathrm{A}| \tag{4}$$

By convention, turns to the right are defined as positive heading change ($\Delta\psi > 0$) and turns to the left as negative heading change ($\Delta\psi < 0$).

Given a turn direction for each aircraft that is manoeuvring and a specified heading change corresponding to a chosen time to turn, t_1, the present authors want to determine the separations between aircraft A and B while they are turning for $t < t_1$ and then while the aircraft are flying along straight-line segments after completing their turns at t_1. Expressions for the separations for the two cases of interest will be derived here, namely one aircraft, either A or B, manoeuvring or both A and B performing coordinated

manoeuvres. In the following discussion, the position vector along the turn segment is designated by the subscript T and the position vector along the straight-line segment is designated by the subscript S.

A preparatory step in calculating the separations is to determine the position coordinates of aircraft A along the turn arc as a function of the heading-change angle $\Delta\psi_A$. From the geometry of the encounter illustrated in Fig. 1, the following expression for the position vector $\boldsymbol{P}_{AT}$ as a function of $\Delta\psi_A$ is obtained

$$\boldsymbol{P}_{AT} = \boldsymbol{R}_{CA} + \boldsymbol{R}_{\Delta\psi_A} \tag{5}$$

where $\boldsymbol{R}_{CA}$ is the vector of length R_A pointing from the initial position of A to the centre of the turn and $\boldsymbol{R}_{\Delta\psi_A}$ is the vector of length R_A pointing from the centre of the turn at C_A to the point on the turn circle where the aircraft is located after turning through an angle $\Delta\psi_A$. After substituting the appropriate expressions for the vector components into equation (5), the following expression for the components of $\boldsymbol{P}_{AT}$ is obtained

$$\boldsymbol{P}_{AT} = R_A \,\mathrm{sgn}(\Delta\psi_A)\,[1 - \cos\Delta\psi_A, \sin\Delta\psi_A] \equiv [x_A, y_A] \tag{6}$$

The signum function, sgn, with argument $\Delta\psi_A$ has been inserted in order to combine separate expressions for right and left turns into a single expression applicable to both turn directions.

Next, the position vector $\boldsymbol{P}_{BT}$ of aircraft B is determined as a function of $\Delta\psi_B$, which can be written as

$$\boldsymbol{P}_{BT} = \boldsymbol{P}_{B0} + \boldsymbol{R}_{CB} + \boldsymbol{R}_{\Delta\psi_B} \tag{7}$$

where $\boldsymbol{P}_{B0} = (x_{B0}, y_{B0})$ denotes the initial position vector of B.

With the help of Fig. 1, expressions for the components of $\boldsymbol{R}_{CB}$ and $\boldsymbol{R}_{\Delta\psi_B}$ can be derived when B is turning through an angle $\Delta\psi_B$ from an initial heading of ψ_B. This yields the following expression

$$\begin{aligned}\boldsymbol{P}_{BT} = [&x_{B0} + R_B \,\mathrm{sgn}(\Delta\psi_B)\,\cos\psi_B \\ &- R_B \,\mathrm{sgn}(\Delta\psi_B)\,\cos(\psi_B + \Delta\psi_B), \\ &y_{B0} - R_B \,\mathrm{sgn}(\Delta\psi_B)\,\sin\psi_B \\ &+ R_B \,\mathrm{sgn}(\Delta\psi_B)\,\sin(\psi_B + \Delta\psi_B)] \equiv [x_B, y_B]\end{aligned} \tag{8}$$

As before, the signum function allows a single expression to be used for representing both right- and left-turn manoeuvres.

Single aircraft and cooperative resolution manoeuvres require separate analyses for determining the separations during turns. Assuming only A manoeuvres while B continues to fly along its initial heading, the coordinates of B are determined at the time A has turned through an angle $\Delta\psi_A$. Then the coordinate vector of B and its components at any time t are

$$\begin{aligned}\boldsymbol{P}_{BS} = \boldsymbol{P}_{B0} + t\boldsymbol{V}_B = [&x_{B0} + tV_B \sin\psi_B, \\ &y_{B0} + tV_B \cos\psi_B] \equiv [x_B, y_B]\end{aligned} \tag{9}$$

The time to turn is obtained by solving the first of equations (3) for t.

The desired expression for the separation d_A during the turn for aircraft A manoeuvring is obtained by taking the absolute value of the difference vector between P_{BS} and P_{AT}

$$d_A = \sqrt{\begin{aligned}&[x_{B0} + tV_B \sin\psi_B - R_A \mathrm{sgn}(\Delta\psi_A) \\ &\times (1 - \cos\Delta\psi_A)]^2 + [y_{B0} + tV_B \cos\psi_B \\ &- R_A \mathrm{sgn}(\Delta\psi_A) \sin\Delta\psi_A]^2\end{aligned}} \tag{10}$$

Similarly, the separation d_B for aircraft B manoeuvring while A continues in a straight line can be written as

$$d_B = \sqrt{\begin{aligned}&[x_{B0} + R_B \,\mathrm{sgn}(\Delta\psi_B) \cos\psi_B - R_B \,\mathrm{sgn}(\Delta\psi_B) \\ &\times \cos(\psi_B + \Delta\psi_B)]^2 + [y_{B0} - t\,V_A - R_B \,\mathrm{sgn}(\Delta\psi_B) \\ &\times \sin\psi_B + R_B \,\mathrm{sgn}(\Delta\psi_B) \sin(\psi_B + \Delta\psi_B)]^2\end{aligned}} \tag{11}$$

where the coordinate vector of A is given by

$$\boldsymbol{P}_{AS} = t\boldsymbol{V}_A = [0.0,\ t\,V_A] \equiv [0.0,\ y_A] \tag{12}$$

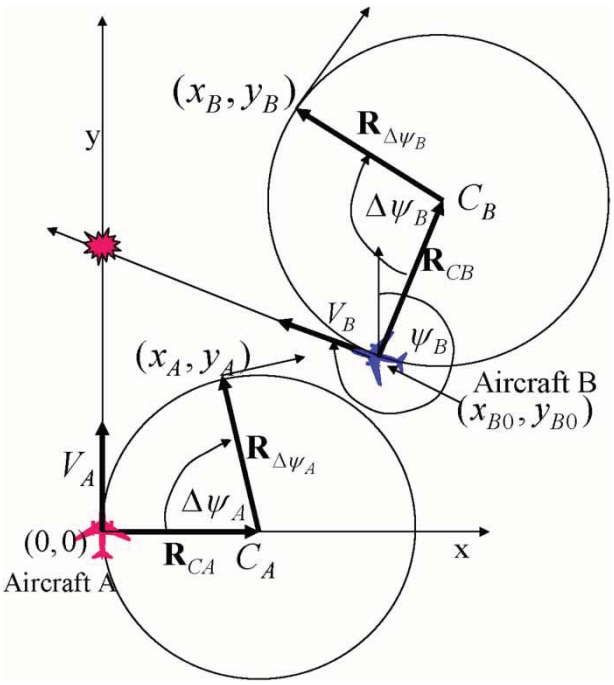

Fig. 1 Illustrating the coordinate system and parameters for resolution manoeuvres

Finally, for the case of cooperative manoeuvres the separation during the turns, d_{AB}, is

$$d_{AB} = \sqrt{\begin{aligned}&[x_{B0} + R_B \operatorname{sgn}(\Delta\psi_B)\cos\psi_B - R_B \operatorname{sgn}(\Delta\psi_B)\\ &\times \cos(\psi_B + \Delta\psi_B) - R_A \operatorname{sgn}(\Delta\psi_A)\\ &\times(1 - \cos\Delta\psi_A)]^2 + [y_{B0} - R_B \operatorname{sgn}(\Delta\psi_B)\\ &\times \sin\psi_B + R_B \operatorname{sgn}(\Delta\psi_B)\sin(\psi_B + \Delta\psi_B)\\ &- R_A \operatorname{sgn}(\Delta\psi_A)\sin\Delta\psi_A]^2\end{aligned}} \tag{13}$$

It should be noted that in the expression for d_{AB}, the relationship between the turn angles $\Delta\psi_A$ and $\Delta\psi_B$ is given by equation (4). Also, equations (10), (11), and (13) can be simplified by combining terms and using well-known trigonometric identities.

The next step is determining the separation along the straight-line flight segments after the turns have been completed. Here it is observed that in the straight-line segments only the minimum separation is of interest, since this value is sufficient to determine whether the resolution manoeuvre will achieve the required separation.

Let $d_{s\min}$ designate the minimum separation in the straight-line segment, t_s designate a value of elapsed time measured from the end of the turn(s) at time t_1, and $t_{s\min}$ designate the value of t_s, where the minimum separation is reached. While there are several ways to derive expressions for $t_{s\min}$ and $d_{s\min}$, the derivation is approached by using the condition that, at the time and location where the minimum is reached, the position difference vector and the relative-velocity vector between A and B, respectively, must be perpendicular to each other. This condition is equivalent to requiring that the dot product of these vectors must be zero at that time. Defining the difference vector as $\boldsymbol{D}_S$ and the relative velocity vector as $\boldsymbol{V}_R = \boldsymbol{V}_B - \boldsymbol{V}_A$, the condition for minimum separation thus becomes

$$\boldsymbol{D}_S \cdot \boldsymbol{V}_R = 0 \tag{14}$$

Define the position coordinates of A and B at the start of the straight-line flight as (x_{A1}, y_{A1}) and (x_{B1}, y_{B1}) and the heading angles as ψ_{A1} and ψ_{B1}, respectively. The position coordinates at the end of the turns can be obtained from equations (6) and (8) after the resolution turn angle(s) $\Delta\psi_{A1}$ and $\Delta\psi_{B1}$ at t_1 have been specified. The position difference and relative vectors can now be written as a function of known quantities

$$\begin{aligned}\boldsymbol{D}_S = [&x_{B1} - x_{A1} + t_s(V_B\sin\psi_{B1} - V_A\sin\psi_{A1}),\\ &y_{B1} - y_{A1} + t_s(V_B\cos\psi_{B1} - V_A\cos\psi_{A1})]\end{aligned} \tag{15}$$

$$\begin{aligned}\boldsymbol{V}_R = [&V_B\sin\psi_{B1} - V_A\sin\psi_{A1},\\ &V_B\cos\psi_{B1} - V_A\cos\psi_{A1}]\end{aligned} \tag{16}$$

where $\psi_{A1} = \Delta\psi_A$ and $\psi_{B1} = \psi_B + \Delta\psi_B$.

These expressions are now substituted into the vector dot product, equation (14), and the resulting linear equation is solved for $t_s = t_{s\min}$. To simplify the resulting expression, recurring parameters are defined as follows

$$\begin{aligned}\Delta_{x1} &= x_{B1} - x_{A1}\\ \Delta_{y1} &= y_{B1} - y_{A1}\\ V_{Rx} &= V_B\sin\psi_{B1} - V_A\sin\psi_{A1}\\ V_{Ry} &= V_B\cos\psi_{B1} - V_A\cos\psi_{A1}\end{aligned} \tag{17}$$

Then the following expression is obtained for $t_{s\min}$

$$t_{s\min} = \frac{-(\Delta_{x1}V_{Rx} + \Delta_{y1}V_{Ry})}{|\boldsymbol{V}_R|^2} \geqslant 0 \tag{18}$$

A zero value for $t_{s\min}$ implies that the minimum separation occurs at the beginning of the straight-line segment. A negative value implies that the separation at an infinitesimal angle before the end of the turn must have been less than the minimum separation at the end of the turn. This characteristic is discussed further in the next section.

The components of the separation vector at $t_{s\min}$ can now be obtained by replacing t_s in equation (15) with the expression for $t_{s\min}$ from equation (18). Then the absolute value of this vector yields the minimum separation in the straight-line segment

$$d_{s\min} = \sqrt{\begin{aligned}&\left[\Delta_{x1} - \frac{V_{Rx}(\Delta_{x1}V_{Rx} + \Delta_{y1}V_{Ry})}{|\boldsymbol{V}_R|^2}\right]^2\\ &+ \left[\Delta_{y1} - \frac{V_{Ry}(\Delta_{x1}V_{Rx} + \Delta_{y1}V_{Ry})}{|\boldsymbol{V}_R|^2}\right]^2\end{aligned}} \tag{19}$$

It should be noted that $t_{s\min}$, measured relative to t_1, can be expressed relative to zero time at the start of the manoeuvre by adding t_1 to $t_{s\min}$. In the following sections, computer-generated solutions to equations (10), (11), (13), (18), and (19) are used to gain insight into the characteristics of the resolution trajectories and to devise an algorithm that generates resolution manoeuvres for arbitrary initial conditions.

4 RELATIONSHIP BETWEEN RESOLUTION MANOEUVRES AND MINIMUM SEPARATIONS

In this section, the relationships between initial conditions and the corresponding minimum separations that resolution manoeuvres can achieve are explored. In addition to providing an understanding of the characteristics of the resolution process, these relationships will contribute to the development of a robust and efficient algorithm for generating resolution manoeuvres. The specification of a resolution manoeuvre to resolve a conflict using the formulation

of the preceding section depends on five initial conditions and the bank angle. The five initial conditions are the speed of aircraft A and the two position coordinates, the heading and the speed of aircraft B. Here it is recalled that in this formulation the initial position and heading of B are specified relative to the initial position and heading of A. Since the coordinates of A and B are usually given in a rectangular coordinate system with the y-axis facing North, the relative initial coordinates of B can be computed by a coordinate transformation.

A resolution manoeuvre is specified by giving the direction of turn for each aircraft, the heading change angle and the bank angle. Since each aircraft can turn right or left and may turn by itself or in cooperation with the other aircraft, each value of heading-change angle thus generates eight different manoeuvres. Assuming that any of the eight manoeuvre types is specified, it will be determined how the separations in the turns given by equations (10), (11), or (13), and the minimum separations in the straight-line segments given by equations (18) and (19) depend on the heading-change angle. Let $d_T(\Delta\psi)$ represent the minimum separation in the turn as given by any of the three separation functions in equations (10), (11), or (13), and let $d_{s\,min}(\Delta\psi)$ be the minimum separation in the straight-line segment after the turn. Then the lower bound of separation as a function of turn angle $d_{min}(\Delta\psi)$ can be generated by performing the following minimizing operation at each value of the argument

$$d_{min}(\Delta\psi) = \min_{d_T, d_{s\,min}} [d_T(\Delta\psi),\ d_{s\,min}(\Delta\psi)] \tag{20}$$

The extrema of $d_{min}(\Delta\psi)$ are important in that they establish the limits of separation that can be achieved with turns in a specified direction.

Before examining the extrema of equation (20) for an example conflict later in this section, some general properties of the constituent functions of equation (20) will be derived first. These properties impose constraints on the behaviour of equation (20) for any conflict scenario or initial condition, and are stated below as theorems.

Theorem 1

Divide the resolution angle interval $\Delta\psi_{min} \leqslant \Delta\psi \leqslant \Delta\psi_{max}$ into non-overlapping subintervals of negative, zero, and positive slope of the function d_T. This is possible because d_T is a differentiable function of $\Delta\psi$, which may have one or more local extrema or possibly inflection points where the slope is zero. Then it follows that in subintervals where the slope is positive, $d_{s\,min} = d_T$. In other words, within this range of resolution angles the $d_{s\,min}$ tracks the d_T function.

Proof

A positive slope indicates that as a straight-line segment is increased from zero length at the end of the turn to a short non-zero length, the separation must increase. Since the function for the separation in the straight-line segment has only one minimum, this implies that the length of the straight-line segment that achieves $d_{s\,min}$ must be zero and its value must therefore be identical to d_T.

Theorem 2

In intervals where the slope of d_T is negative, $d_{s\,min} < d_T$.

Proof

A negative slope indicates that as a straight-line segment increases from zero to a short non-zero length, the separation decreases. Thus, the minimum of the separation in the straight-line segment occurs at some non-zero distance from the end of the turn, and its minimum separation must therefore be less than d_T. This conclusion follows from the fact that the separation function in the straight-line segment can have at most one minimum.

Theorem 3

At the extremum points (or possibly points of inflection) of d_T where the slope is zero, $d_{s\,min} = d_T$.

Proof

A zero slope indicates that an infinitesimal length of straight-line segment at the end of the turn neither increases nor decreases the separation. This condition defines the minimum of the separation function and implies that $d_{s\,min}$ is achieved at zero length. Hence $d_{s\,min} = d_T$ at such points.

Theorem 4

$$d_{s\,min}(\Delta\psi) \leqslant d_T(\Delta\psi) \forall \Delta\psi$$
$$\text{such that } \Delta\psi_{min} \leqslant \Delta\psi \leqslant \Delta\psi_{max}$$

where $\Delta\psi_{min}$ and $\Delta\psi_{max}$ define the range of user-specified resolution angles. Thus, the value of the function d_T places an upper bound on the function $d_{s\,min}$ for any chosen $\Delta\psi$. This follows directly from theorems 1–3.

Alternatively, the truth of theorem 4 also follows from the definition of the locus of $d_{s\,min}$, which cannot have a value greater than the separation at the end of the turn. That value corresponds to a straight-line segment of zero length.

These characteristics are illustrated in Fig. 2, which shows examples of d_T and $d_{s\,min}$ plotted as functions of $\Delta\psi$. The locus of d_T exhibits the cyclic variation that is typical for this function. The locus of $d_{s\,min}$ has been drawn so as to obey the four characteristics proven in

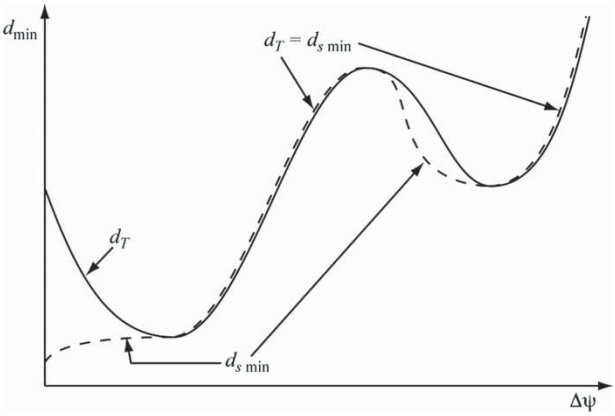

Fig. 2 Locus of minimum separation as a function of the lower bound of d_T and $d_{s\,min}$

the theorems above. It shows that the locus of $d_{s\,min}$ merges with the locus of d_T at points of minimum separation in the turn and diverges from the common locus of the two functions at the maximum of d_T. Knowing that all such loci must conform to these characteristics is helpful both for giving a succinct description of the separation behaviour and for detecting and debugging errors in automatically generated plots of separation functions for example conflicts.

5 ANALYSIS OF RESOLUTION CHARACTERISTICS USING SEPARATION GRAPHS

In this section, the structure of resolution trajectories will be determined by analysing a specific conflict encounter using a graphical representation similar to that shown in Fig. 2. Although only one example is analysed, the method developed for this example will serve as a template for analysis of a large class of encounters. It is used in the next section to develop general resolution rules for any encounter as well as for creating a computer algorithm for generating resolutions. For each conflict encounter, a representation of resolution trajectories in coordinates of separation versus turn angle allows the graphical display of all possible resolution trajectories for a specified turn direction.

The representation of Fig. 2 will be expanded on by using the left half of the coordinate plane to represent left-turn trajectories and the right half to represent right-turn trajectories. In addition, the effect of bank angle will be included by plotting the separations for bank angles of 15°, 20°, 25°, and 30°, which were chosen because they span the range typically used in airline manoeuvres. In the graphs, the time to reach minimum separation for the 30° bank angle case is also included. Thus, one composite graph gives the separation outcomes for all possible resolution choices. These outcomes are given as functions of turn direction, turn angle, bank angle, and time. However, a single composite graph does have the limitation of representing only one of the two aircraft performing the manoeuvre. Therefore, a second composite graph is required to represent the other aircraft performing the manoeuvre. To complete the analysis of separations for an encounter, two additional composite graphs are required for the coordinated manoeuvre case. In summary, four sets of composite graphs provide sufficient information for the complete analysis of each conflict encounter.

Computer code and plotting routines were developed to generate the composite graphs automatically for any conflict encounter. The expressions that determine the separations used in plotting the composite graphs are the two separation equations, d_T and $d_{s\,min}$. In addition, the time to reach minimum separation as a function of turn angle is automatically generated and plotted. In the computer code, the user also specifies the discrete values of turn angle at which the separations are generated. The graphs presented in this article used 2.5° increments, which were sufficient to produce smooth curves for all quantities that are graphed.

The conflict analysed using this graphical representation is shown in Fig. 3. The upper left shows the initial location and heading of the conflict aircraft along with two example resolution manoeuvres. Aircraft B is initially at the coordinate (12 and 12.5), and its intercept angle with the manoeuvring aircraft A is 90°. The turn radii are drawn approximately to scale, and they represent bank angles of 15° and 30°. The vertical axis on the left of the graph uses a single scale calibration for both nautical miles of separation and minutes to minimum separation.

At 0° turn angle, the graph shows three important parameters of the conflict, namely, the initial distance between the conflict aircraft (17 nmi), the minimum separation without manoeuvring (2 nmi), and the time to minimum separation (∼1.8 min). The solid lines show the separation as a function of the turn angle for the four values of bank angle. Note that by entering the composite graph at a chosen value of turn angle, turn direction, and at one of the discrete values of bank angle, one can read off the graph both the separation during the turn and the minimum separation in the straight-line segment, if one exists, following the turn.

For turns to the right, the heading-change angles that achieve the minimum separation during the turns vary from about 65° at a bank angle of 15 to 90° at a bank angle of 30°. The minimum separations during the turns increase with increasing bank angle from about 5.5 nmi to about 8.5 nmi. As required by theorem 3 of the previous section, the loci of minimum separations in the straight-line segments (dashed curves) intercept the loci of separation in the turn at the heading-change angles where the separations

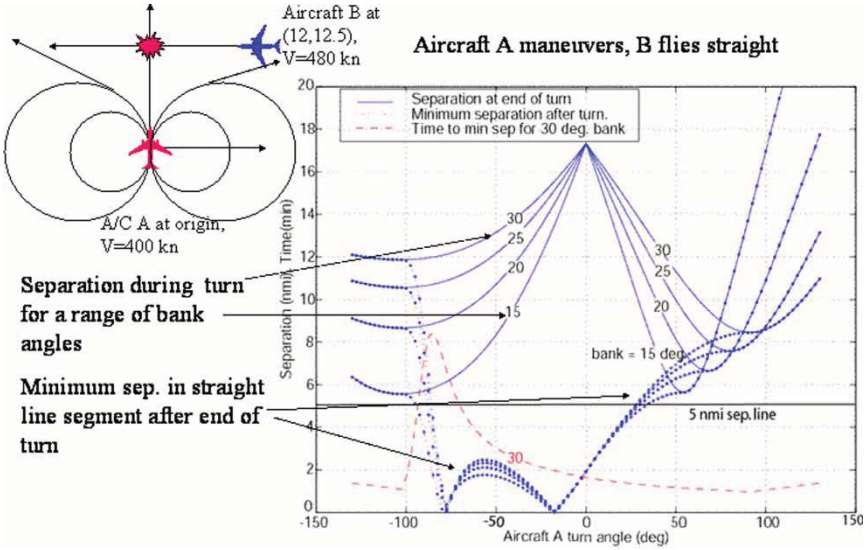

Fig. 3 Separation versus turn angle for conflict with 90° encounter angle

in the turns are at a minimum. After the loci have joined at the minimum separation points, they form a single locus, as required by theorem 1. For turns to the right, the loci of minimum separations increase monotonically with heading-change angle. In this conflict encounter, turns to the right by aircraft A cause it to cross the path of aircraft B behind aircraft B. Such a manoeuvre is sometimes referred to as a back-side resolution. It is preferred by controllers, because it produces stable and predictable resolutions. This finding is confirmed by the graphical results.

The situation is considerably more complex for turns to the left. Small turns followed by straight-line flight produce decreasing minimum separations for any bank angle, finally resulting in a collision at a heading-change angle of about 20°. Surprisingly, the turn angle resulting in zero separation is essentially independent of the bank angle. Thereafter, the minimum separation increases with heading-change angle until it reaches a maximum at 60°. Then it plunges again to a collision point at about 80° turn angle. Past this second collision angle, the minimum separation in the straight-line segment rises rapidly with increasing turn angle until its locus merges with that of the separation in the turn, which occurs at the angle producing minimum separation. The turn angle producing minimum separation in the turn, which occurs at about 103°, is seen to be nearly independent of the bank angle for bank angles between 15° and 30°.

Investigation of smaller bank angles (not presented here) has shown that the turn angle yielding minimum separation in the turn begins to change at bank angles <10°. However, the minimum separation is a fairly sensitive function of the bank angle, increasing from 5.5 nmi at 15° bank angle to 11.8 nmi at 30° bank angle. Finally, the locus of time to minimum separation is observed to rise to a sharp peak of 8.5 min at about 85° and then to fall rapidly to a minimum of 1 min at an angle of 103°, which coincides with the angle of minimum separation in the turn.

The complex behaviour of the separation loci, as illustrated by the left-turn manoeuvres in this example, requires care in the selection of resolution turn angles to reduce the risk of failure in resolving the conflict. Therefore, turn angles equal to or greater than those that give the maximum separation in the straight-line segment and smaller than those that give the minimum in the turn will not be used for resolution manoeuvres. The separation locus in this range is in an unstable region in the sense that small changes in turn angle can result in large changes in minimum separation. As the example illustrates, it is possible that a relatively small increase in the turn angle can produce a sharp decrease in minimum separation.

The turn direction that causes the manoeuvring aircraft to cross the path of aircraft B in front of aircraft B (in this example the left-turn direction) is referred to as a front-side resolution. Its unstable and sensitive separation behaviour with respect to turn angles often makes these manoeuvres less desirable than the back-side manoeuvres. The unstable behaviour of front-side resolutions is exacerbated in this example by the fact that the speed of the manoeuvring aircraft is less than that of the non-manoeuvring aircraft.

An important use of the composite graphs is for graphically determining resolution manoeuvres that meet specified separation criteria and for detecting by inspection when the criteria cannot be met. To illustrate how this is done, assume that the required separation must be at least 5 nmi. Draw a line across the graph at the 5 nmi separation value, as shown in Fig. 3. Locate the points where the line intersects the separation loci and read off the corresponding turn angles. For turns to the right, a 35° heading change at a

15° bank angle yields the specified separation. Slightly smaller heading changes are required for the higher bank angles. In this resolution the minimum separation is reached in the straight-line segment after the turn.

For turns to the left at a bank angle of 15°, a heading-change angle of 103°, followed by straight-line flight, will yield a minimum separation of about 5.5 nmi. Higher values of bank angle will achieve even higher minimum separations. Heading changes >103° followed by straight-line flight also give acceptable resolutions, but they will not increase the minimum separation, which is reached in the turn at 103° for the 15–30° bank angle range studied. Note that the graph also shows that a solution giving exactly 5 nmi of separation is obtained for a left turn with heading change of about 80°. However, this solution falls in the region of unstable separation with respect to turn angle at any of the plotted bank angles, and therefore must be avoided.

To complete the analysis of this conflict scenario, the separation results for the remaining six manoeuvre types must be generated. The six additional types comprise the two manoeuvre directions for aircraft B and the four manoeuvre directions for cooperative manoeuvres. The graphs for the eight manoeuvre types are shown in the four sets of composite graphs of Fig. 4. The resolution analysis of this conflict scenario can now be completed by using Fig. 4 to determine all the manoeuvre types and corresponding turn angles that will meet or exceed a specified value of 5 nmi minimum separation. Considering first manoeuvres by aircraft B alone, the graphs (upper right, Fig. 4) show that a heading change to the right of about 22° at any bank angle between 15° and 30° will yield a minimum separation of 5 nmi in the straight-line segment after the turn. For single aircraft manoeuvres, this resolution is optimum in the sense that it uses the least heading change to achieve the desired minimum separation.

Finally, turning attention to the cooperative manoeuvre graphs at the bottom of Fig. 4, it is found that three types of manoeuvres provide acceptable resolutions at any bank angle between 15° and 30°. These are A turning left and B turning right, A turning right and B turning right, and both A and B turning left. It is noted that for the cooperative manoeuvre graphs, only the turn angle of aircraft A is plotted in the horizontal axis. The corresponding turn angle of aircraft B can be calculated from equation (4). Of these three types of cooperative manoeuvres, the type 'A right and B right' achieves the required separation with the

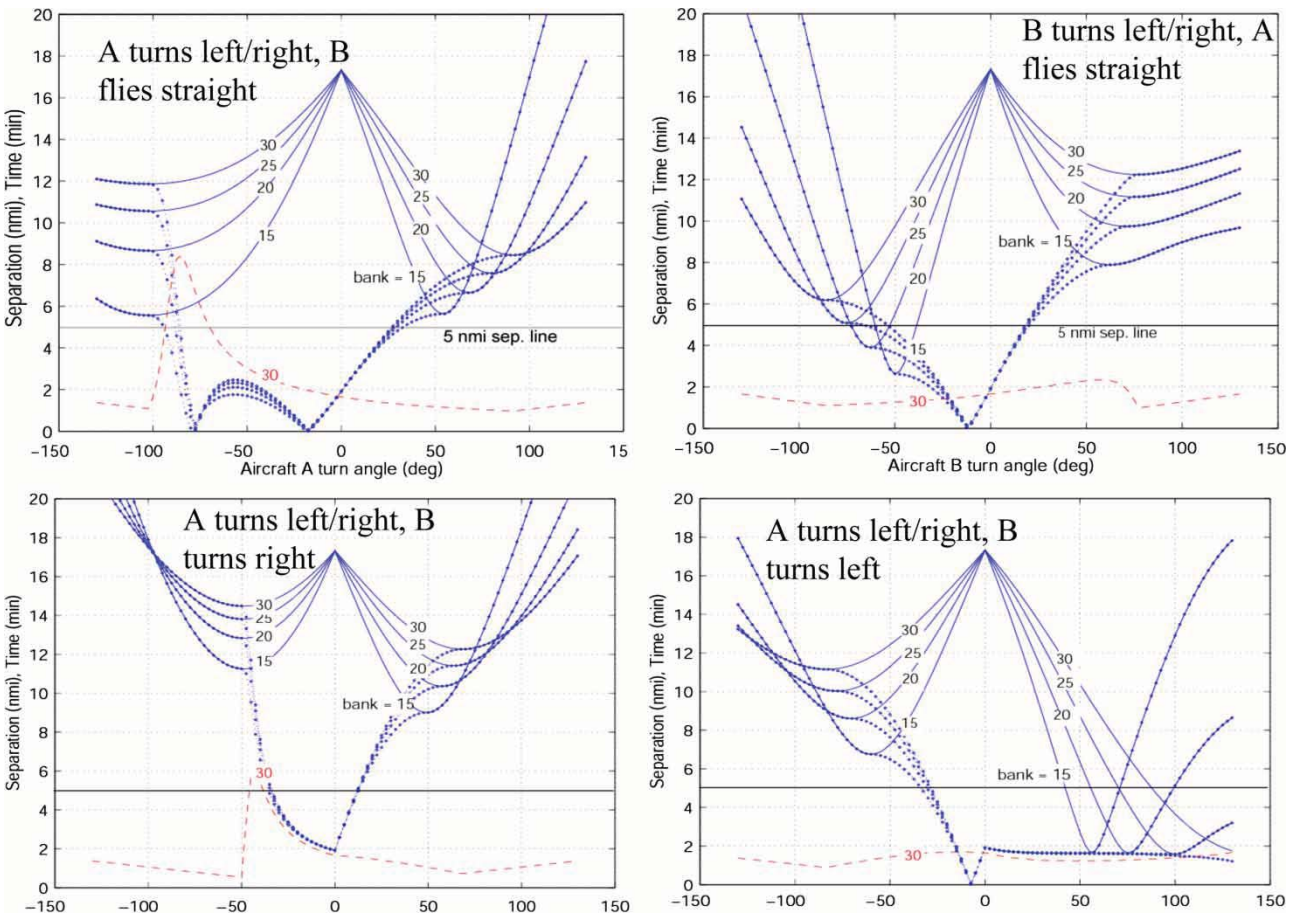

Fig. 4 Separation graphs for eight manoeuvre types; the same conflict scenario as in Fig. 3

least heading change (about 15°), with respect to both single aircraft and cooperative manoeuvres. The only manoeuvre type that yields unacceptable resolutions is A right and B left. The separation graphs for this manoeuvre type show that a nearly constant value of minimum separation of slightly <2 nmi is achieved over a wide range of heading-change angles. The choice of bank angle has little effect on this minimum.

The method of analysis described here for one example has been applied to a set of conflict scenarios that broadly span the range of possible encounters. The conflicts studied included encounter angles ranging from near head-on to near in-trail and initial separations ranging from 2 min to loss of separation to as short as 30 s from a collision. Analysis of the separation graphs for this set identified a few additional characteristics not present in the example conflict. These characteristics, which occur for certain special initial conditions, have been catalogued and are accounted for in the design of the computer code for generating resolution manoeuvres. One such characteristic is a discontinuity in the locus of minimum separation in the straight-line segment. The discontinuity occurs where the two separation loci converge at the heading-change angle for minimum separation in the turn. The discontinuity, which occurs only for certain initial conditions and when the two aircraft are flying at the same speed, does not contradict the theorems proved earlier.

6 DESIGN OF RESOLUTION ALGORITHM

The preceding sections have focused on elucidating the separation characteristics of resolution trajectories with constraints on the bank angle. Knowledge of these characteristics is used in this section to help design an algorithm that generates safe and efficient manoeuvres for resolving short-range conflicts. The design objective for the algorithm is to generate resolution manoeuvres for any conflict scenario, including encounters that would result in collisions within <1 min if not promptly and effectively resolved. The algorithm is intended for implementation in a ground-based system that sends a resolution manoeuvre automatically via ground-air data to the aircraft in a conflict. With appropriate modifications it could also be used in an air-to-air conflict-avoidance system that operates independently of the ground. In either implementation a synthesized aural advisory in the cockpit would instruct the pilot to make a specified heading change in a specified direction with either a standard turn rate or an expedited turn rate. The option to choose from two levels of turn rates, which correspond to standard and high bank angles, allows the algorithm to incorporate the severity and urgency of the conflict in the resolution manoeuvre. This approach should be acceptable to pilots who are accustomed to receiving controller clearances with 'expedite' in the message of controller-pilot communications.

After examining the range of bank angles airline pilots typically use in performing heading-change manoeuvres, 15° and 30° were chosen as representative of standard and high bank angle turns, respectively. It is not suggested – nor is it necessary – that pilots turn exactly at the assumed bank angles in order for the manoeuvre to successfully resolve a conflict. When generating the resolution manoeuvre, the algorithm compensates for the variability in bank angle/turn rate by incorporating buffers in the required minimum separation. Such buffers will reduce the sensitivity of the manoeuvre to a pilot's actual choice of bank angle.

In broad outline, the algorithm first attempts to resolve a conflict with only one aircraft in the conflict pair performing the manoeuvre at the standard bank angle. In the following discussion, a successful resolution is defined as a manoeuvre that maintains the separation above a specified minimum, which is typically assumed to be 5 nmi in en route airspace and 3 nmi in terminal-area airspace. If more than one manoeuvre from among the four possible ones is found that achieves or exceeds the required separation, the algorithm ranks the eligible resolutions in order of least heading change. If it fails to find an eligible manoeuvre among the four manoeuvre types, the algorithm attempts to generate resolutions at the high bank angle. If none is found, the algorithm searches the four types of cooperative manoeuvres for a resolution that achieves or exceeds the required separation at the high bank angle. If no cooperative resolution is found that avoids loss of separation at the high bank angle, the algorithm selects the cooperative manoeuvre that maximizes the minimum separation in the turn. Choosing a manoeuvre that maximizes the minimum separation if loss of separation is unavoidable minimizes the exposure of the conflict aircraft to a potential collision. It provides the safest manoeuvre in the horizontal plane that re-establishes the required separation.

The computational procedure that is fundamental to generating the resolutions involves determining the minimum separation achieved in the turn and the range of the minimum separations achievable in the straight-line segments after a turn. These computations are performed for eight single aircraft manoeuvre types, four of them at standard bank angle and four at high bank angle. If none of these eight manoeuvre types resolves the conflict without loss of required minimum separation, the algorithm generates four cooperative manoeuvre types using the high bank angle.

Examination of graphs of separation loci, such as those in Fig. 4, for a wide range of conflict encounters has made it possible to characterize the behaviour of the separation loci into a limited number of behaviour

types. In general, the shorter the time to loss of separation, the more unusual the loci are likely to behave. From an analysis of the behaviour types, a computational approach has evolved that generates acceptable resolution manoeuvres for any conflict scenario.

For a selected turn direction and bank angle, the algorithm first calculates the minimum separation in the turn, defined as $d_{T_{min}}$, and the corresponding heading change angle, $\Delta\psi_{T\,min}$, from equations (10), (11), or (13). If $d_{T\,min} \geqslant d_{req}$, where d_{req} is the required separation, a turn angle $\Delta\psi_{req}$ is known to exist such that $d_{min} = d_{req}$ and $0 < \Delta\psi_{req} \leqslant \Delta\psi_{T\,min}$. The corresponding manoeuvre using this turn angle achieves a minimum separation that is equal to the required separation in the straight-line segment after the turn of angle $\Delta\psi_{req}$ has been completed. The value of $\Delta\psi_{req}$ is obtained by setting the left side of equation (19) equal to d_{req} and solving the resulting expression for $\Delta\psi_{req}$. The actual process for finding the solution is explained next.

As has been seen above, the minimum separation locus generated by equation (19) can show diverse behaviour that depends on the manoeuvre type and the conflict parameters. Thus, the approach to solving equation (19) for $\Delta\psi_{req}$ must be able to adapt to the different behaviour categories, both simple and complex. For example, for the right-turn manoeuvres in Fig. 3 the $d_{s\,min}$ locus increases monotonically from $\Delta\psi = 0$ and then merges smoothly with the turn locus at $\Delta\psi = \Delta\psi_{T\,min}$. This behaviour ensures that a solution can be easily found. On the other hand, the complex behaviour of the locus for left-turn manoeuvres requires careful attention to the method for solution. In order to handle both monotonic- and complex-behaving loci with multiple extrema (minimums and maximums), the algorithm first evaluates $d_{s\,min}$ in small increments of turn angle $\Delta\psi$ in order to locate the extrema (minimums and/or maximums) of the locus before it merges with the angle locus at $\Delta\psi_{T\,min}$.

If the minimum separation for the null manoeuvre is not zero, as is typically the case, the first extremum can be either a minimum or a maximum. It will be a minimum if $d_{s\,min}$ is initially decreasing as $\Delta\psi$ is incremented and a maximum otherwise. If it is a minimum, the angles ranging from zero to the minimum are excluded from consideration as resolution turn angles, because angles in this region would give even lower separations than the null manoeuvre. Moreover, if the turn angle for the first minimum occurs at $\Delta\psi = \Delta\psi_{T\,min}$, then the manoeuvre type corresponding to this turn direction does not have an acceptable solution and is abandoned. Otherwise, the angles are incremented past the first minimum until the maximum is reached.

The first maximum may be found either when $\Delta\psi < \Delta\psi_{T\,min}$ or when $\Delta\psi = \Delta\psi_{T\,min}$. If the former is true, this is a case similar to that for the left turn in Fig. 3. In that case, compare the maximum of $d_{s\,min}$ with d_{req}. If $d_{req} \leqslant d_{s\,min}$ at its maximum, it is known that an angle $\Delta\psi$ exists such that $d_{s\,min} = d_{req}$. This unknown angle can be determined by standard iterative procedures for solving non-linear equations. If $d_{req} > d_{s\,min}$ at its maximum, no solution exists in the angle range between the minimum and the maximum of $d_{s\,min}$. If that is the case, the last chance for finding a solution for this manoeuvre type is to determine if $d_{req} \leqslant d_{T\,min}$. If that is the case, an acceptable solution is found at $\Delta\psi = \Delta\psi_{T\,min}$. Otherwise, the manoeuvre type under consideration has no solution that yields a minimum separation equal to or greater than d_{req}.

The solution at $\Delta\psi_{T\,min}$ will generally yield a minimum separation that is larger than d_{req}, since it is likely that $d_{req} < d_{T\,min}$ and not exactly equal to $d_{T\,min}$. Note that the turn-angle interval that is bounded from below by the angle $\Delta\psi$ at which $d_{s\,min}$ is maximum and above by $\Delta\psi < \Delta\psi_{T\,min}$ is excluded because it is in the unstable resolution range, as previously explained.

The algorithm described previously attempts to find resolutions that minimize the heading change to achieve the required separation. Minimizing the heading change is operationally desirable because it helps to reduce the deviation from the original flight path, thereby minimizing the time delay introduced by the manoeuvre. These types of resolutions are referred to as type 1 in the flow chart of the algorithm shown in Fig. 5. However, under certain conditions, resolution manoeuvres that minimize the heading change may require excessive amounts of time to reach the minimum separation point in the straight-line segment.

This effect can be seen in Figs 3 and 4 by examining the plots of time to reach minimum separation as a function of turn angle for the 30° bank angle case. In

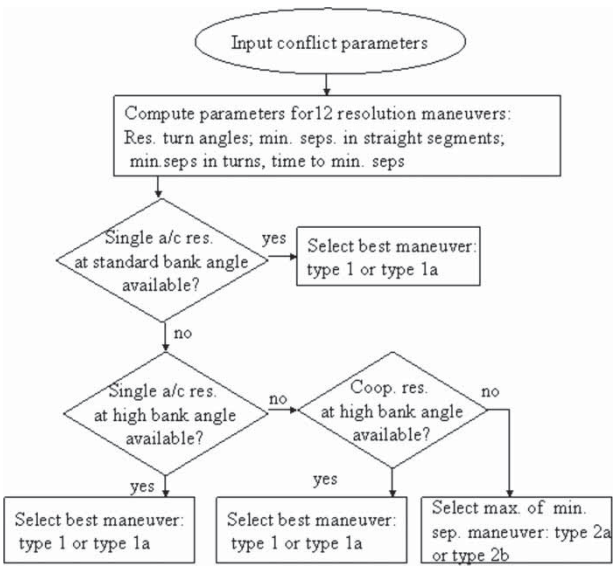

Fig. 5 Flow chart of resolution algorithm

the case of the left turn, the time to minimum separation begins to rise sharply about halfway to the $\Delta\psi_{\mathrm{T\,min}}$ turn angle. For resolutions of some conflicts, it is even possible for the time to approach infinity. Examination of the geometry of resolution manoeuvres exhibiting this behaviour indicates that it occurs when the straight-line segment after the turn becomes nearly parallel to the path of the other aircraft. Such manoeuvres can take an unreasonably long time to reach the minimum separation point. Another undesirable feature of such manoeuvres is their sensitivity to the heading angle in the region of steeply increasing time. To avoid these undesirable characteristics, the algorithm includes logic that modifies the resolution manoeuvre if the time to completion becomes excessive. To determine if the time is excessive, the logic computes the time to reach the minimum separation in the straight-line segment at angle $\Delta\psi_{\mathrm{req}}$ and the time to turn to d_{req}.

If the time to reach minimum separation in the straight-line segment at angle $\Delta\psi_{\mathrm{req}}$ exceeds the time to $\Delta\psi_{\mathrm{T\,min}}$ by a specified percentage, then the logic substitutes $\Delta\psi_{\mathrm{T\,min}}$ for $d_{\mathrm{req}} > d_{\mathrm{s\,min}}$. A value of 20 per cent for the specified percentage achieves a reasonable compromise between time to turn to $d_{\mathrm{s\,min}}$ and minimizing the heading-change angle. This value was used to generate the example resolutions in Table 1 to be discussed later. Manoeuvres that use $\Delta\psi_{\mathrm{T\,min}}$ as the resolution turn angle are referred to as type 1a resolutions. This type generally achieves a minimum separation $d_{\mathrm{T_{min}}}$ that is larger than the required separation.

The next procedure performed by the algorithm is to sort the attempted resolution manoeuvres in preference order. The set of attempted resolutions always contains 12 manoeuvres consisting of eight single aircraft types at standard and high bank angle and four cooperative manoeuvres at high bank angle. Manoeuvres that meet or exceed the required separation are listed first. Manoeuvres that fail to achieve the required separation are also included and labelled as failed. The 12 attempted resolutions are separated into three sub-tables, one for standard bank angle, one for high bank angle, and one for cooperative manoeuvres at high bank angle. Typically, each sub-table contains more than one acceptable manoeuvre. The redundancy in acceptable manoeuvres can be used to satisfy additional manoeuvre constraints. Such additional constraints may include, but are not limited to, an inability to manoeuvre the preferred aircraft or the presence of a close-by third aircraft. Each row in a sub-table specifies the manoeuvre type and the parameters for the resolution. The first listed resolution in each sub-table is generally the one that requires the least heading change (type 1). It can also be a type 1a, as explained earlier.

Finally, the algorithm determines a manoeuvre of last resort to be used when the three sub-tables contain no resolution manoeuvres that achieve separations equal to or greater than the required minimum separation. This situation can occur either when aircraft are so close at the time the conflict is first detected that loss of separation has already occurred or when loss of separation cannot be prevented by any type of turn manoeuvre with limits on the bank angle. Under such conditions the requirements for a resolution manoeuvre change from resolving a conflict to first avoiding a collision and then re-establishing legal separation. To handle such severe conflicts, the algorithm implements a two-stage strategy for generating a manoeuvre. It selects from the sub-table of four cooperative manoeuvres the manoeuvre that maximizes the minimum separation while both aircraft are turning. This type of manoeuvre is considered the safest one possible under the circumstances. The second stage of this manoeuvre is to choose an end-of-turn heading that is greater than $\Delta\psi_{\mathrm{T\,min}}$. This heading is chosen to correspond to the turn angle that achieves the required separation. The angle is found by the same iterative procedure previously described for the other resolutions. At this angle the aircraft is clear of the conflict and begins its straight-line flight. Because of the characteristics of the separation functions stated as theorem 4 earlier, the separation will increase monotonically after the start of the straight-line segment. This resolution manoeuvre, if it exists, is identified as a type 2a resolution in Fig. 5.

However, it is possible that no turn angle $>\Delta\psi_{\mathrm{T\,min}}$ will be found such that the required separation is achieved while turning up to and including the angle that gives the maximum separation in the turn. Under those conditions, the turns are terminated at the angle where the separation in the turn is at a maximum. Again, it is known from theorems 1 and 4 that the separation will continue to increase monotonically in the straight-line segment after the turn. This type of resolution is identified as type 2b in the resolution algorithm flow chart (Fig. 5). The cooperative manoeuvre turn direction at high bank angle that gives the maximum of the minimum separations during the turns is the first manoeuvre listed in the corresponding sub-table.

Table 1 gives the resolution manoeuvres and the associated parameters calculated by the algorithm for the conflict scenario illustrated in Fig. 3. The first sub-table for single aircraft manoeuvres at 15° bank angle shows that three manoeuvre types achieve acceptable resolutions. The A-straight–B-left manoeuvre requires the smallest heading change (22.5°) of the three successful manoeuvres and is therefore listed at the top, although the other manoeuvres provide equally acceptable alternatives. The second sub-table for 30° bank angle shows that all four manoeuvre types give acceptable resolutions. For the A straight, B right and A right, B straight manoeuvres, the algorithm selects a type 1a turn that corresponds to the angle of minimum separation in the turn, $\Delta\psi_{\mathrm{T\,min}}$, rather than a type 1

Table 1 Resolution manoeuvres for conflict with initial configuration: $V_A = 400$ knots, $V_B = 480$ knots, $\psi_B = 270°$, $x_{B0} = 12$ nmi, and $y_{B0} = 12.5$ nmi

		Resolution parameters			Minimum separation in turn		
Turn directions	Turn type	Turn angle (°)	Time (min)	Minimum separation (nmi)	Turn angle (°)	Time (min)	Minimum separation (nmi)
Bank angle 15°. Single aircraft manoeuvres							
A straight, B right	1	22.5	1.90	5.0	62.5	1.71	7.9
A right, B straight	1	35.0	1.32	5.0	55.0	1.26	5.6
A left, B straight	1a	102.5	2.35	5.6	102.5	2.35	5.6
A straight, B left	2a failed	62.5	1.37	2.6	50.0	1.37	2.6
Bank angle 30°. Single aircraft manoeuvres							
A straight, B left	1	55.0	1.23	5.0	85.0	1.10	6.2
A straight, B right	1a	77.5	0.99	12.3	77.5	0.99	12.3
A right, B straight	1a	92.5	0.98	8.5	92.5	0.98	8.5
A left, B straight	1a	102.5	1.09	11.9	102.5	1.09	11.9
Bank angle 30°. Cooperative manoeuvres							
A left, B right*	1a	50.0	0.53	14.5	50.0	0.53	14.5
A right, B right	1a	67.5	0.74	12.3	67.5	0.74	12.3
A left, B left	1a	82.5	0.90	11.2	82.5	0.90	11.2
A right, B left	2a failed	212.5	1.70	1.3	160.0	1.70	1.3

*Maximum–minimum manoeuvre.

Table 2 Resolution manoeuvres for conflict with initial configuration: $V_A = 400$ knots, $V_B = 480$ knots, $\psi_B = 270°$, $x_{B0} = 4$ nmi, and $y_{B0} = 5.83$ nmi

		Resolution parameters			Minimum separation in turn		
Turn directions	Turn type	Turn angle (°)	Time (min)	Minimum separation (nmi)	Turn angle (°)	Time (min)	Minimum separation (nmi)
Bank angle 30°. Cooperative manoeuvres							
A left, B right*	2a	70.0	0.74	4.5	47.5	0.50	4.5
A right, B right	2a	60.0	0.64	4.2	40.0	0.43	4.2
A right, B left	2a	82.5	0.87	1.8	50.0	0.53	1.8
A left, B left	2a	107.5	1.14	1.6	60.0	0.65	1.6

*Maximum–minimum manoeuvre.

turn to $\Delta\psi_{req}$. This choice is made because the time to reach minimum separation in the straight line segment after turning to $\Delta\psi_{req}$ exceeds the time to turn to $\Delta\psi_{T\,min}$ by more than the requisite 20 per cent. As previously stated, the choice of 20 per cent for switching from type 1 to type 1a manoeuvre, although somewhat arbitrary, represents a reasonable trade-off between time to turn and heading change.

Results for the cooperative resolutions at 30-degree bank angle, shown in the third sub-table, show that three manoeuvre types provide successful resolutions, all of which achieve minimum separations far in excess of the required separation. Based on the procedure described previously, the selection algorithm chooses the preferred resolution as the first entry in Table 1, for which aircraft A flies straight and aircraft B turns 22.5° right with a bank angle of 15°.

Table 2 gives the resolution manoeuvre for the same conflict scenario as in Fig. 3 but with time advanced by 1 min. In this case the conflict aircraft have moved so close to each other that loss of separation cannot be avoided even when using a cooperative manoeuvre at the 30° bank angle. Here, the maximum–minimum solution provides the safest available manoeuvre, which is given in the first line of Table 2 and shown in bold print. This manoeuvre achieves a minimum separation of 4.5 nmi. The second best manoeuvre is only slightly worse at 4.2 nmi minimum separation, and it could be used as an alternative.

7 OUTLINE OF A PROCEDURE FOR AVOIDING SECONDARY CONFLICTS

Before it is accepted as a safe resolution, a candidate resolution trajectory must be checked to find out whether it inadvertently creates new near-term conflicts with other aircraft operating in the immediate vicinity of the two primary conflict aircraft. Such unintended conflicts, which are called secondary

conflicts, must be avoided. They are more likely to occur at high traffic density. In this section, the procedure incorporated into the algorithm is outlined to check for and avoid secondary conflicts.

It is assumed that the algorithm is provided with a list of the current positions, speeds and headings of nearby aircraft that could create secondary conflicts. Such a list can be generated by identifying all traffic within a specified range and altitude of the conflict pair. The next step is to check whether the candidate trajectory will cause loss of separation with any aircraft in the secondary conflict list. This check for secondary conflicts is done by reusing the previously derived separation equations. Thus, for each aircraft in the secondary conflict list, the separation during the turn and the minimum separation in the straight-line segment after the turn are calculated.

A preparatory step for this calculation is to first transform the initial position and heading of each secondary aircraft into the reference frame defined by the initial position and heading of the manoeuvring aircraft using an orthogonal coordinate transformation. This establishes the manoeuvring aircraft as aircraft A and the non-manoeuvring secondary conflict aircraft as aircraft B.

From the known heading change angle of aircraft A, equations (6), (9), (10), (18), and (19) can now be used to calculate the minimum separation and the time when the minimum is reached for each aircraft in the list. The next step is to compare these times and minimum separations with the parameters that define a secondary conflict. Two parameters, d_{reqs} and $t_{\min s}$, are used to define a secondary conflict. A secondary conflict occurs if separation falls below d_{reqs} within a time of $t_{\min s}$ of the start of the resolution manoeuvre. Typical values for these parameters are 5 nmi and 3 min, respectively.

The final step is to modify the original choice of preferred resolution trajectory such that all detected secondary conflicts are avoided. The first choice here for an alternate resolution is to turn the resolution aircraft in the opposite direction. Table 1 is checked to find out if such a resolution is available. If it is, the secondary conflict check for this turn direction is repeated. If no secondary conflicts remain for this turn direction, an acceptable resolution trajectory has been found. If secondary conflicts remain or if opposite turning direction resolution trajectories are not available, Table 1 is checked to find out whether resolutions are available for the other primary conflict aircraft. The process of checking is repeated whether the secondary conflicts can be avoided for the available turn directions for the other aircraft. Continue evaluating the available alternative resolutions at the higher bank angles and for the cooperative resolutions as necessary to avoid all secondary conflicts.

As the density of traffic increases, it is possible that the procedure outlined here fails to resolve all secondary conflicts. In that case vertical resolution manoeuvres may be necessary to avoid secondary conflicts that cannot be avoided by horizontal manoeuvres alone. Another option is to generate additional horizontal resolutions by increasing the resolution turn angles beyond the minimum values given in Table 1. A final option is to choose the resolution that maximizes the minimum separation within $t_{\min s}$ with respect to the remaining unresolved secondary conflicts.

Figure 6 illustrates how a secondary conflict can be avoided by turning beyond the minimum angle for resolving the primary conflict. The primary conflict scenario is that depicted in Fig. 3 and Table 1 for aircraft A and B. Figure 6(a) is a planar view, in which the initial positions of A, B and a potential secondary

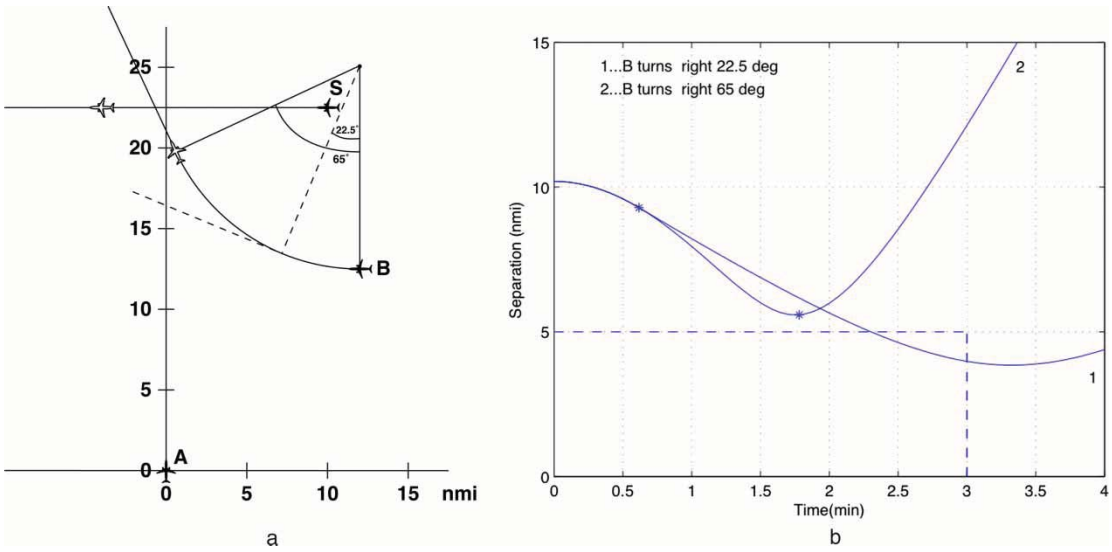

Fig. 6 Separation versus time for secondary conflict

conflict aircraft S are shown as solid symbols. Aircraft S has a velocity of 480 knots, heading 270° and initial coordinates $x = 10$ nmi and $y = 22.5$ nmi. The curves in Fig. 6(b) show the separation of B and S, as a function of time, measured relative to the beginning of the primary conflict resolution manoeuvre. The dashed lines in Fig. 6(b), at separation 5 nmi and time 3 min, outline the region defining loss of separation for secondary conflicts. Trajectories entering this region produce a secondary conflict. Curve 1 represents aircraft B in the primary conflict resolution manoeuvre shown on the first line of Table 1, a 22.5° right turn. The asterisk symbol on the curve marks the end of the turn, after which the separation was calculated using straight trajectories for both B and S. It is seen that, for this manoeuvre, loss of separation occurs between 2.2 and 3 min, with a minimum separation of 3.8 nmi.

The separation of the secondary at the end of the turn determines whether increasing the heading change of B has the potential to avoid the secondary conflict. Only if the end of turn separation is greater than the required separation, as is the case in this example, is it worthwhile to test whether additional heading change can eliminate the secondary conflict. Curve 2 shows the effect of extending the aircraft B turn to 65°, the angle at which the B versus S separation during the turn has a minimum value. This value was chosen as the minimum turn at which the separation can only increase in the following straight-line segment. It is seen that, with this extended turn, the minimum B versus S separation is increased to 5.6 nmi, and the secondary conflict is avoided. In Fig. 6(b), open aircraft symbols show the positions of B and S at the time of minimum separation in this extended manoeuvre.

The basic algorithm for primary conflict resolution has been extended to perform the procedures illustrated in this example for any set of potential secondary conflict aircraft.

8 OPERATIONAL CONCEPT FOR ACTIVE TSAFE

Prior research on TSAFE has focused primarily on developing a reliable method for detecting conflicts at close range, defined as those with 2 min or less to loss of separation. The detection algorithm has been implemented in software and tested extensively using radar track records and operational error reports [**5**]. The automated detection and display of conflicts to controllers will be referred to as TSAFE Alert. With TSAFE Alert, controllers retain responsibility for formulating resolutions and taking action to resolve conflicts. The next step is to send the TSAFE Alert information into a system for generating resolution manoeuvres and give that system the authority to resolve conflicts independently of the controller. This capability is referred to as TSAFE Resolution. TSAFE Resolution constitutes a fundamental change in the role of controllers, since it relieves them of the responsibility for resolving short-range conflicts under agreed-upon conditions.

An operational concept is proposed here that gives TSAFE Resolution the authority to resolve conflicts without impeding a controller's ability to control and manage traffic at the strategic level. The objective of the concept is to reduce a controller's workload associated with short-range separation assurance, thereby giving a controller more time for formulating strategic decisions. TSAFE Resolution plays the role of a safety net that takes action independent of the controller only when it is needed to avoid imminent loss of separation. Controllers would continue to manage traffic at both the short-range (tactical) and long-range (strategic) time scales as they do in the current system. Although TSAFE Resolution and TCAS operate independently of each other, they provide analogous functions for controllers and pilots, respectively, in that the former protects controllers against loss of separation while the latter protects pilots against collisions.

Since the proposed concept allows controllers to handle traffic by using traditional procedures, it is essential to specify the precise conditions under which the responsibility to resolve conflicts shifts from controller to TSAFE Resolution (Fig. 7). The transition process is illustrated in Fig. 7, which shows a timeline of events for both the alerting and resolution functions of TSAFE.

TSAFE Alert would initially display a message on the controller's monitor when a conflict with <2 min to loss of separation has been detected for a pair of aircraft. The message identifies the conflict aircraft to the controller by flashing their respective data tags, the same as Conflict Alert does in the current system. In addition, TSAFE Resolution displays the turn direction and heading change of the intended resolution manoeuvre on the data tag(s) of the conflict aircraft. As long as the time to loss of separation remains >1 min, the controller can choose from the following three options: (1) inhibit TSAFE Resolution from issuing a resolution advisory for the current conflict;

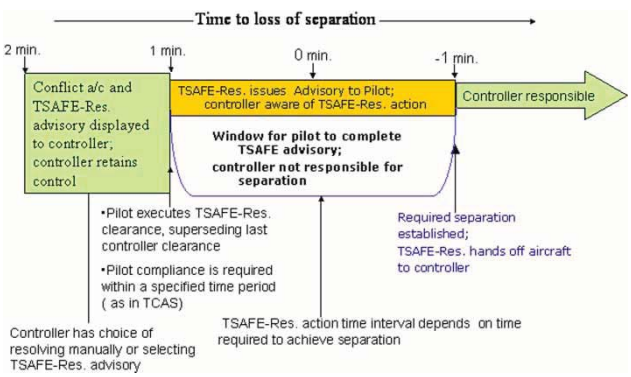

Fig. 7 TSAFE resolution decision timeline

(2) command TSAFE Resolution to issue a resolution advisory to the aircraft; and (3) take no action at the current time.

If the controller chooses the first option, he/she takes responsibility for resolving the conflict manually without the help of TSAFE Resolution. If the controller chooses the second option, TSAFE Resolution immediately sends a resolution advisory to the aircraft. However, in the event that time to loss of separation falls below 1 min without the controller having chosen the first or second option, responsibility for resolving the conflict defaults automatically to TSAFE Resolution. In that circumstance, TSAFE Resolution issues a resolution advisory to the aircraft immediately. The TSAFE advisory would supersede the most recently issued controller clearance.

The 1 and 2 min time intervals referred to in the discussion of TSAFE Resolution should not be regarded as the fixed and final values of these intervals. These intervals reflect estimates based on analysis of time scales encountered in operational systems such as TCAS and Conflict Alert. They are applicable only for en route airspace. In terminal-area airspace, the corresponding values would be about one half of those for en route airspace, or 30 s and 1 min, respectively. Real-time simulations of the concept must be conducted to determine the optimum values for these intervals. Nevertheless, the estimated values are believed to be reasonably close to operationally acceptable values.

It is also possible for TSAFE Alert to detect a conflict with < 1 min to loss of separation. In that event TSAFE Resolution immediately issues a resolution advisory to the aircraft and simultaneously informs the controller that an advisory was issued. Such an action is taken in the interest of safety when it is likely that there is insufficient time for the controller to prevent loss of separation. If the TSAFE Resolution advisory does not succeed in preventing loss of separation for a late-detected conflict, controllers would generally not be held responsible for the separation violation.

There is an exception to this rule. If the immediate cause for the loss of separation is a controller clearance issued within <1 min of the time when the loss of separation occurred, and that clearance is determined to be the immediate cause of the loss of separation, then the controller will be responsible for the loss of separation. Such incidents, referred to as operational errors, are generally caused by controllers unintentionally issuing improperly formulated clearances to an aircraft that is near another aircraft. However, controllers would not be penalized for deliberately allowing time to loss of separation to fall below 1 min, thereby causing TSAFE Resolution to resolve the conflict.

After the pilot has executed the resolution manoeuvre and separation is assured, the controller assumes responsibility for returning the aircraft to its pre-resolution flight plan. A message on the controller's monitor indicates when the aircraft has cleared the conflict and control of the aircraft is handed off to the controller.

It is proposed that both horizontal and vertical manoeuvres for resolving conflicts be incorporated into TSAFE Resolution. Although the algorithm described earlier was developed specifically to meet the performance requirements of TSAFE Resolution, a system that integrates both types of resolution manoeuvres must still be developed. While both types of manoeuvres will be available for resolving conflicts, horizontal manoeuvres may be less likely to trigger or interfere with TCAS resolution alerts, since TCAS is limited to only vertical manoeuvres. Restricting TSAFE Resolution advisories to horizontal manoeuvres may also reduce the potential for pilots to become confused by the two types of advisories. Similar to TCAS, TSAFE Resolution advisories will be enunciated to the cockpit crew via synthesized aural messages. TSAFE–TCAS interaction issues and methods for avoiding undesirable interference between them have recently been studied in reference [**9**].

It is hypothesized that the operational implementation of TSAFE Resolution in the NAS would result in reductions in controller workload while also increasing safety. The combination of these benefits would allow controllers to handle more traffic and thereby increase airspace capacity.

9 HUMAN FACTORS ISSUES

From a human factors perspective, low-frequency events that have high consequence for safety of flight if not detected in a timely manner are especially appropriate targets for handling by an automated system. Automation of such events is less likely to result in 'skill' loss by controllers. Skill loss is more likely to occur when a controller is unable to maintain awareness of the traffic situation as a whole and to anticipate traffic operations in a 'strategic/tactical' time frame. Since the action of TSAFE Resolution is limited to handling events requiring immediate response, it is not likely to produce 'skill loss' when the responsibility for handling such events is shifted from controller to automation.

Knowledge of intent increases the controller's situational awareness. Compared to TCAS, which gives no advance indication of its intent or action to the controller, TSAFE informs the controller that an advisory has been issued at the same time the advisory is uplinked to the flight crew. This feature should ameliorate, if not eliminate, the difficulties controllers occasionally experience when resuming control of an aircraft after a TCAS resolution has been performed.

Both controllers and pilots will need to understand the TSAFE role and the conditions under which TSAFE

advisories are issued. As in TCAS, pilot compliance within a specified time period will be required. Procedures must be defined that make the handoff from TSAFE back to the controller after separation has been established unambiguous to both the controller and the pilot. Pilots need to be trained to respond to TSAFE and to understand the difference in the conditions that trigger either a TSAFE or TCAS alert.

The important issue of controller acceptance of the operational concept must be examined in a real-time simulation with both controllers and pilots in the loop. Such a simulation is being planned for the near future.

10 DATA-LINK REQUIREMENTS FOR TSAFE RESOLUTION

An essential requirement for implementing TSAFE Resolution in the NAS is the availability of an appropriate ground-air data link. Such a data link must be able to uplink TSAFE Resolution advisories to the conflict aircraft securely and with little delay.

Since a data link between the ground and aircraft is the main enabler of TSAFE Resolution, the availability and performance of a data link in the NAS for this application must be examined. The most promising technology for this application is the data link incorporated in the Mode S surveillance system [**10**, **11**]. The performance of the data link incorporated into Mode S, referred to as Mode S Specific Services, appears to meet the requirements of TSAFE Resolution. Mode S is embedded in the infrastructure for TCAS on-board passenger aircraft and is thus available for operational use in the NAS. By reusing the existing TCAS infrastructure, only minor modifications to existing on-board systems would be needed in order to deploy TSAFE Resolution.

The Mode S Specific Services is an International Civil Aviation Organization (ICAO)-approved data-link protocol that was designed for message exchanges between the ground and aircraft. Several unused channels with both standard and extended message length are available for use by TSAFE. A standard-length Comm A message transmitted at 1030 MHz is entirely adequate for uplinking TSAFE Resolution manoeuvres. The Comm A message is 112 bits long, of which 56 bits contain the payload wherein the resolution-manoeuvre parameters are inserted. The available bit length is greater than what is required for specifying a resolution manoeuvre. The extra bits can be used to uplink the identity and location of the other conflict aircraft and to encode the message with redundant bits in order to reduce transmission errors.

The data-link message protocol includes 24-bit parity-error detection, which is built into the transponder of the receiving aircraft. If the received message passes the parity check, the aircraft acknowledges the reception of the message by sending a handshake reply back to the ground at 1090 MHz. If the handshake reply is not received, the ground assumes that the message was not received and resends the message. The parity-error check reduces the probability of an undetected transmission error by a factor of $\sim 10^7$.

While this error rate is already very low, an additional procedure can be implemented to check the correctness of the message received by the aircraft. For this purpose the ground initiates a message read-back request to the conflict aircraft using the Ground Initiated Comm B (GICB) message, which is also 112 bits long. The conflict aircraft responds to this request by sending a copy of the resolution message stored in the TSAFE-dedicated register of the transponder back to the ground at 1090 MHz. By comparing the read-back message with the original uplinked message, the ground system can definitively establish whether or not the resolution manoeuvre was correctly received by the aircraft and, if not, resend the original Comm A resolution message. In addition, the ground system can initiate a GICB message to read back the current TCAS alert status and resolution parameters. TSAFE can use knowledge of the TCAS alert status to avoid incompatible or redundant resolution advisories. The sequence of Comm A and GICB message exchanges between ground and conflict aircraft is illustrated in Fig. 8.

The resolution and read-back message exchange occurs during the brief time interval when the direction-sensitive Mode S sensor is aligned with the direction of the receiving aircraft. This alignment occurs periodically at the rotation interval of the Mode S sensor. Since the sensor rotates along with the surveillance radar antenna, the rotation rate is 12 s for en route and 4.6 s for terminal-area radars. Thus, the latency in uplinking a resolution message is at most 12 s, which is considered to be acceptable for TSAFE Resolution.

The GICB and Comm A protocols are a standard part of all the Mode S sensors in the NAS and they are also standard in nearly all Mode S transponders. It is important to note that the Mode S Specific Services data link is currently used operationally in the NAS to support the 'Traffic Information Service' as defined in reference [**10**]. Furthermore, Eurocontrol mandates support of GICB in all transponders in its airspace by 2009 as part of the elementary surveillance and enhanced surveillance applications. Also, read-out of TCAS resolution advisories using GICB data link has been demonstrated multiple times in experimental applications. Therefore, as an available technology both in the ground system and in the aircraft, the Mode S Specific Services Data Link is exceptionally well suited to support a safety-critical system such as TSAFE Resolution.

Although the Mode S Specific Services technology is mature and ready for use, it is not currently

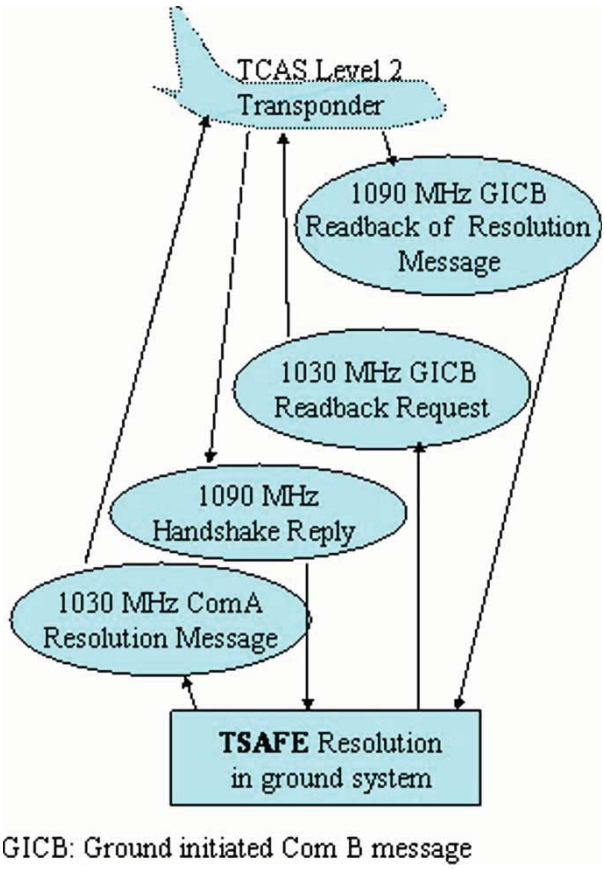

Fig. 8 Mode S Specific Services message exchange for TSAFE Resolution

implemented in the NAS. Specifically, the surveillance system of the NAS would have to be upgraded to process Specific Services messages of the type required to support TSAFE Resolution. The required upgrade consists primarily of software functions that would have to be inserted into a future build of FAA's En Route Automation Modernization (ERAM) system.

Recently, FAA initiated an effort to develop new specifications for a future data link, referred to as Data Com. If the FAA's future Data Com technology achieves the fast access and high reliability required for delivering safety-critical messages, it could be used instead of Mode S for TSAFE Resolution.

11 CONCLUDING REMARKS

Given the initial positions and velocities of a pair of aircraft in conflict, the resolution algorithm developed in this article generates the minimum separations for all eight combinations of turn directions at a specified bank angle. The analytical model that generates the separations is computationally efficient and does not require potentially time-consuming iterative procedures. Therefore, the algorithm is well suited for real-time implementation.

The graphical representation of solutions in the parameter space of turn angle, separation during a turn, and minimum separation in the straight-line segment after the turn provided the key to revealing the characteristics of resolution manoeuvres as a function of initial conditions. Analysing this parameter space over ensembles of conflict scenarios gave a comprehensive picture of the resolution characteristics. The picture that emerged was used to specify logical and computational procedures that allow the algorithm to generate the safest possible resolution manoeuvres for any conflict scenario, including those that would result in collisions within less than a minute. The resolution method built into the algorithm is therefore well suited for TSAFE Resolution and could also find use in a collision-avoidance system such as TCAS.

The primary enabling function for TSAFE Resolution is the availability of a reliable ground–air data link. The data link available in Mode S has the requisite performance and functionality to support this concept. Since Mode S is already used throughout the world as an element of TCAS, the opportunity exists for installing the airborne element of TSAFE Resolution at relatively low cost to airline operators. The resolution algorithm of TSAFE must be adapted by the FAA for insertion into the future ground-based system, known as ERAM, whose deployment is in progress. However, before considering an implementation strategy for this concept it is essential to conduct studies and real-time simulations that can assess the safety- and capacity-improving potential of TSAFE Resolution.

The operational concept for TSAFE, comprising alerting and resolution functions, performs as an autonomous agent with responsibility to resolve near-term conflicts that are overlooked by a controller or are handed off to the agent by the controller. It can be viewed as a critical first step in shifting responsibility for ensuring separation from the controller to an automated agent. Such a paradigm shifting step is likely to expose complex human-factor issues that have to be studied analytically and in humans-in-the-loop simulations.

ACKNOWLEDGEMENTS

The author gratefully acknowledges the contribution of Professor Kevin Corker to the human factors analysis of TSAFE. His insights into controller and pilot acceptance of the proposed concept have been invaluable. Much of the analysis of human factor issues in this article is based on a presentation he made to the authors in July and August 2007. Professor Corker lost his battle with cancer in January 2008. He is greatly missed as a friend and colleague.

REFERENCES

1 **Erzberger, H.** Transforming the NAS: the next generation air traffic control system. In Proceedings of the International Congress of the Aeronautical Sciences (ICAS), Yokohama, Japan, 30 August 2004.

2 **Erzberger, H.** Automated conflict resolution for air traffic control. In Proceedings of the 25th International Congress of the Aeronautical Sciences, Hamburg, Germany, September 2006.

3 **Farley, T.** and **Erzberger, H.** Fast time air traffic simulation of a conflict resolution algorithm under high air traffic demand. In Proceedings of the USA Europe ATM Seminar, paper 173, Barcelona, Spain, 2–5 July 2007.

4 **Paielli, R. A.** and **Erzberger, H.** Tactical conflict detection methods for reducing operational errors. *Air Traffic Control Q.*, 2005, **13**(1), 83–106.

5 **Paielli, R. A.** and **Erzberger, H.** Tactical conflict alerting aid for air traffic controllers. *AIAA J. Guid. Control Dyn.*, 2009, **32**(1), 184–193.

6 **Paielli, R. A.** Modeling maneuver dynamics in air traffic conflict resolution. *AIAA J. Guid. Control Dyn.*, 2003, **26**(3), 407–415.

7 **Mitchell, I. M., Bayen, A. M.,** and **Tomlin, C. J.** A time-dependent Hamilton-Jacobi formulation of reachable sets for continuous dynamic games. *IEEE Trans. Autom. Control*, 2005, **50**(7), 947–957.

8 **Clements, J. C.** Optimal simultaneous pairwise conflict resolution maneuvers in air traffic management. *AIAA J. Guid. Control Dyn.*, 2002, **25**(4), 815–818.

9 **Tang, H., Denery, D., Erzberger, H.,** and **Paielli, R. A.** Tactical separation assurance algorithm and impacts of airborne collision avoidance system. In Proceedings of the AIAA Guidance and Control Conference, Honolulu, Hawaii, 18–21 August 2008, AIAA paper 2008-6973.

10 RTCA DO-239. Minimum Operational Performance Standards for Traffic Information Service (TIS) Data Link Communications; issued 2 April 1997. Document available from RTCA, Inc., Washington D.C., USA, www.rtca.org.

11 **Grappel, R. D., Harris, G. S., Kozar, M. J.,** and **Wiken, R. T.** Elementary surveillance and enhanced surveillance validation via mode S secondary radar surveillance. MIT Lincoln Laboratory Report ATC-337, Cambridge, Massachusetts, January 2008.

APPENDIX

Notation

$\boldsymbol{C}$	position vector for centre of the turn
d	separation
d_{smin}	minimum separation in straight line segment
d_{T}	minimum separation in turn
$\boldsymbol{D}$	difference vector
g	acceleration of gravity
$\boldsymbol{P}$	position vector
R	turn radius
$\boldsymbol{R}$	position vector
t	time
t_1	time at end of turn
$t_{\text{s min}}$	time at minimum separation
V	airspeed
x	position coordinate in a rectangular (stereographic pseudo-Cartesian) coordinate system
y	position coordinate in a rectangular (stereographic pseudo-Cartesian) coordinate system
ϕ	bank angle
ψ	heading angle